American Mineralogist, Volume 93, pages 1903–1910, 2008

Lakargiite $CaZrO_3$: A new mineral of the perovskite group from the North Caucasus, Kabardino-Balkaria, Russia

Evgeny V. Galuskin,[1,*] Viktor M. Gazeev,[2] Thomas Armbruster,[3] Aleksander E. Zadov,[4] Irina O. Galuskina,[1] Nikolai N. Pertsev,[2] Piotr Dzierżanowski,[5] Milen Kadiyski,[3] Anatoly G. Gurbanov,[2] Roman Wrzalik,[6] and Antoni Winiarski[6]

[1]Faculty of Earth Sciences, Department of Geochemistry, Mineralogy, and Petrography, University of Silesia, Będzińska 60, 41-200 Sosnowiec, Poland
[2]Institute of Geology of Ore Deposits, Geochemistry, Mineralogy, and Petrography (IGEM), Russian Academy of Sciences, Staromonetny 35, 119017 Moscow, Russia
[3]Mineralogical Crystallography, Institute of Geological Sciences, University of Bern, Freiestrasse 3, CH-3012 Bern, Switzerland
[4]OOO NPP TEPLOHIM, Dmitrovskoye av., 71, 127238 Moscow, Russia
[5]Institute of Geochemistry, Mineralogy, and Petrology, Warsaw University, al. Żwirki i Wigury 93, 02-089 Warszawa, Poland
[6]August Chełkowski Institute of Physics, University of Silesia, Uniwersytecka 4, 40-007 Katowice, Poland

Abstract

Lakargiite $CaZrO_3$—the zirconium analog of perovskite [*Pbnm*, a = 5.556(1), b = 5.715(1), c = 7.960(1) Å, V 252.7(1) Å^3, Z = 4]—was discovered as an accessory mineral in high-temperature skarns in carbonate-silicate rocks occurring as xenoliths in ignimbrites of the Upper-Chegem (Verkhniy Chegem) volcanic structure, the North Caucasus, Kabardino-Balkaria, Russia. Lakargiite forms pseudo-cubic crystals up to 30–35 μm in size and aggregates up to 200 μm. Lakargiite is associated with spurrite, larnite, calcio-olivine, calcite, cuspidine, rondorfite, reinhardbraunsite, wadalite, perovskite, and minerals of the ellestadite group. The new perovskite mineral belongs to the ternary solid solution $CaZrO_3$-$CaTiO_3$-$CaSnO_3$ with a maximum $CaZrO_3$ content of ca. 93%, maximum $CaTiO_3$ content of 22%, and maximum $CaSnO_3$ content of 20%. Significant impurities are Sc, Cr, Fe, Ce, La, Hf, Nb, U, and Th. Raman spectra of lakargiite are similar to those of the synthetic phase $Ca(Zr,Ti)O_3$ with strong bands at 352, 437, 446, 554, and 748 cm^{-1}. Lakargiite crystallized under sanidinite-facies conditions of contact metamorphism characterized by very high temperatures and low pressures.

Keywords: Lakargiite, perovskite group, solid solution, $CaZrO_3$, $CaSnO_3$, Raman spectroscopy, skarn, Caucasus

Introduction

The natural analog of the well-known orthorhombic synthetic phase $CaZrO_3$ named lakargiite was discovered in altered carbonate xenoliths within ignimbrites in the North Caucasus, Kabardino-Balkaria, Russia (Gazeev et al. 2006).

Perovskite $CaTiO_3$, discovered in 1820 in the Akhmatovskaya Pit, Nazyamskiye Mountains, Zlatoust district, Urals (Rose 1839; Pekov 1998), became the prototype of many synthetic perovskite materials—oxides, hydroxides, fluorides, and other compounds with important and easily modified physical and chemical properties of technical value (Mitchell 2002; Levin et al. 2006).

Eight perovskite-group minerals are known to date. There are titanates and niobates with the crystal chemical formula ABO_3: perovskite $CaTiO_3$ (Rose 1839), loparite $(Na,REE,Ca)_2Ti_2O_6$ (Kuznetsov 1925), lueshite $NaNbO_3$ (Safiannikoff 1959), latrappite $(Ca,Na)(Nb,Fe^{3+},Ti)O_3$ (Nickel 1964), macedonite $PbTiO_3$ (Radusinović and Markov 1971), tausonite $SrTiO_3$ (Vorob'ev et al. 1984), isolueshite $(Na,REE)(Nb,Ti)O_3$ (Chakhmouradian et al. 1997), and barioperovskite $BaTiO_3$ (Ma and Rossman 2008). The classification of the perovskite group is currently open to revision in the light of the discovery of silicate perovskite and the diversity of "fluoroperovskites" (Mitchell 2002). High-pressure silicate perovskite $(Mg,Fe^{2+})SiO_3$ occurs in the Earth's mantle (Saxena et al. 1996).

Synthetic materials produced on the basis of calcium zirconate ($CaZrO_3$) have a broad range of applications, from proton conductors (Iwahara 1996) to ceramics used for immobilization of long-lived radionuclides (Lumpkin 2001). Although $CaZrO_3$ has been proposed as a component of naturally occurring perovskites its content does not exceed 5 mol% (Lupini et al. 1992; Mitchell 2002; Chakhmouradian 2006). The natural analog of $CaZrO_3$ has not been discovered until now in spite of the common enrichment of natural systems in Zr and Ca. This rarity is due to (1) the high crystallization temperature of $CaZrO_3$ and (2) the high activity of Si in many natural systems, which leads to the formation of zircon $ZrSiO_4$, thus decreasing Zr activity in the fluid. Ca-Zr(+Ti)-oxide phases are exemplified by tazheranite $Ca_2Zr_5Ti_2O_{16}$, a cubic modification of ZrO_2 stabilized by Ca and Ti, and by the tetragonal analog of tazheranite-calzirtite found in Si-undersaturated zones in most high-temperature (800–900 °C) skarns (Konev and Samoilov 1974; Galuskin et al. 2007).

Lakargiite $CaZrO_3$, the zirconium analog of perovskite $CaTiO_3$, was approved as a new mineral species in July 2007 (IMA-2007-014) by the Commission on New Minerals, No-

* E-mail: galuskin@us.edu.pl

menclature and Classification (CNMNC) of the International Mineralogical Association (IMA). Lakargiite is an accessory mineral in high-temperature skarns occurring in sedimentary carbonate xenoliths in ignimbrite confined to the Upper-Chegem (Verkhniy Chegem) volcanic structure of the North Caucasus. The mineral name derives from that of Lakargi Mountain. The holotype sample of lakargiite (number 3590/1) is deposited at the Fersman Mineralogical Museum in Moscow.

GEOLOGIC SETTING

The Upper-Chegem volcanic structure (ca. 110 km^2) is situated in the mountainous part of Kabardino-Balkaria (North Caucasus, Russia) on the watershed of the Chegem and Baksan Rivers. The lower part of the Upper-Chegem caldera section comprises a series (<1.5 km thick; 2.8–3.0 Ma) of pinkish-gray ignimbrites and tuffs of rhyolitic and rhyodacitic composition (Borsuk 1979). It is overlain by a 50–60 m thick moraine of the Mindel glaciation. Thin sheets of two-pyroxene andesite occur in the upper part of the rock sequence. Porphyritic granodiorites (~2.5–2.8 Ma; Borsuk 1979; Lipman et al. 1993) build a stock of ca. 15 km^2 at the northern part of the Upper-Chegem volcanic structure.

Some areas with carbonate- and silicate-xenoliths occur within the ignimbrite field near the divide (43.2° N 43.1° E) located between the Lakargi and Vorlan mountain peaks. These xenoliths (<20 m in size) are fragments of Middle- and Upper-Jurassic rocks underlying the Upper-Chegem volcanic structure. The xenoliths are associated with relics of volcanic pipes preserved on the Lakargi and Vorlan peaks (Milanovsky and Koronovsky 1973). The thickness of skarn zones containing lakargiite in the carbonate xenoliths varies from a few decimeters to 1.5 m.

ANALYTICAL METHODS

Determination of lakargiite crystal morphology and selection of single crystals and aggregates for X-ray study and Raman spectroscopic investigations were performed using a scanning electron microscope (Philips/FEI ESEM XL30 with EDS/EDAX). The chemical composition was determined using an electron-microprobe analyzer (CAMECA SX100; 15 kV, 40–50 nA). The lines (and standards) used were Ca$K\alpha$, Si$K\alpha$, Mg$K\alpha$ (diopside), Ti$K\alpha$ (rutile), Cr$K\alpha$ (Cr_2O_3), Al$K\alpha$ (orthoclase), Fe$K\alpha$ (Fe_2O_3), Mn$K\alpha$ (rhodochrosite), Zr$L\alpha$ (zircon), Sn$L\alpha$ (cassiterite), Sc$K\alpha$ (Sc), U$M\beta$ (UO_2), Th$M\alpha$ (ThO_2), Nb$L\alpha$ (Nb), Sr$L\alpha$ (celestine), Hf$M\alpha$ (HfO_2), Ta$M\alpha$ (Ta), Y$L\alpha$ ($Y_3Al_5O_{12}$), La$L\alpha$ (LaP_5O_{14}), Ce$L\alpha$ (CeP_5O_{14}), Nd$L\beta$ (REE4). Corrections were calculated using a PAP procedure provided by CAMECA.

X-ray diffraction data for selected lakargiite crystals were collected using a single-crystal X-ray diffractometer (Bruker SMART CCD) with graphite-monochromated Mo$K\alpha$ radiation.

A powdered sample was examined with a D/max RAPID II X-ray diffractometer from Rigaku with a rotating anode, Ag$K\alpha$ radiation, operated at 60 kV and 200 mA, equipped with $K\alpha$ monochromator and curved imaging plate systems for two-dimensional X-ray scattering. The two-dimensional XRD image was integrated as a function of 2θ to give a conventional one dimensional diffraction profile. Two irregular aggregates of lakargiite (~50 μm) were powdered and formed as a sphere 0.3 mm in diameter using gum arabic. Measurement was performed at room temperature. The X-ray powder-diffraction pattern of the natural material was calculated from the two-dimensional XRD image (Ag$K\alpha_{1,2}$ radiation) using the RAPID XRD program. PowderCell for Windows version 2.4 (Kraus and Nolze 1996), based on the Rietveld method, was used to calculate the lattice parameters of lakargiite. The starting parameters were taken from Koopmans et al. (1983). Because of a strong gum arabic X-ray peak at 6.6° and many overlapping lines at 2θ angles higher than 45°, the spectrum was analyzed in a 2θ range of 10.6–45.0°. A pseudo-Voigt2 peak-shape function was applied for fitting.

Raman spectra were recorded using a LabRam System spectrometer (Jobin-Yvone-Horiba) equipped with a monochromator (1800 line/mm grating), a Peltier-cooled CCD (1024 × 256), and an Olympus BX40 confocal microscope. The incident laser excitation was provided by an air-cooled argon laser source operating at 514.5 nm. The power at the exit of a 50× or 100× objective varied from 20–40 mW. To avoid undesirable Rayleigh scattering, two notch-filters were used that cut the laser line at 200 cm^{-1}. The non-polarized spectra were recorded in 0° geometry, in the range 200–4000 cm^{-1} of Raman shift and with a spectral resolution of 3.5 cm^{-1}. The collection time was 60 s and 10 scans were accumulated. The Raman scattering line of a silicon plate (520.7 cm^{-1}) was used in the routine calibration of the monochromator.

IR spectra were obtained with a Bio-Rad FTS-6000 spectrometer with a micro-ATR accessory (MIRacle) equipped with KRS-5 lenses and a single-reflection diamond ATR. A small amount of sample was simply placed onto the ATR crystal and pressure up to 75 psi applied to the sample. The FT-IR spectra of 32 scans were averaged to obtain the single-beam background- and sample micro-ATR spectra. Spectra were collected from 360 to 6000 cm^{-1} with a resolution of 4 cm^{-1} and were modified to a form approximating the absorbance curves with the aid of ATR correction.

RESULTS

High-temperature mineralization of the skarns is characterized by spurrite, larnite, calcio-olivine, reinhardbraunsite, cuspidine, rondorfite, wadalite, perovskite, calcite, ellestadite-group minerals (Gazeev et al. 2006), as well as lakargiite, and a potentially new mineral, $Ca_3Fe_2TiO_8$. Larnite, calcio-olivine, spurrite, rondorfite, cuspidine, and other minerals characterize and define discrete zones. Later minerals are represented by hillebrandite, afwillite, hydrogarnet, jennite, hydrocalumite, ettringite-group minerals, gypsum, serpentine, allophane, hematite, and bernalite. Barite (Sr-Ca-bearing), kilchoanite, portlandite, fassaitic pyroxene, periclase, galena, stolzite, manganoan sphalerite, native Bi, chalcocite, and zircon occur in minute quantities (Gazeev et al. 2006). The highest concentration of lakargiite occurs in spurrite rocks where lakargiite is confined to rock portions rich in wadalite, hydrocalumite, calcite, and minerals of the ettringite-thaumasite series (Figs. 1a–1c).

Lakargiite occurs as pseudocubic twinned crystals <30–35 μm in size (Fig. 1a) bounded by forms {100} and {111}, skeletal crystals and spherulite-like forms <200 μm (Figs. 1b–1d). Framboid-like lakargiite and lakargiite-hydrocalumite aggregates with a mean grain size of ca. 500 nm are common (Fig. 1e). Skeletal crystals of lakargiite have inclusions of calcite, hydrocalumite, wadalite, minerals of the ettringite-thaumasite series, and various hydrosilicates of calcium (Fig. 1b). Micrometer-size relics of baddeleyite occur in lakargiite aggregates (Fig. 1c). A porous pseudomorph of lakargiite after zircon was found in a cuspidine zone of a rock with relics of volcanic glass (Fig. 1f).

The color of lakargiite crystals varies from red-brown (high Ti contents) to yellowish and almost colorless. In thin section, the color varies from light-brown to colorless. The mineral is not pleochroic. Under reflected light with crossed polars, lakargiite shows characteristic red-brown and pink internal reflections. The color of the powdered mineral varies from light-brown to cream-white. Lakargiite has vitreous to adamantine luster, submetallic for dark varieties. Its hardness is 8–9 (Mohs), microhardness VHN_{100} = 1392–1708 kg/mm^2, mean 1545 kg/mm^2. Cleavages on {110} and {001} (orthorhombic orientation) are well defined, fracture is uneven. Density was not measured because of the small crystal size, high porosity, and abundance of mineral inclusions. Density of 4.587 g/cm^3 was calculated from the mean empirical formula (Mandarino 1981) and the cell volume obtained from powder X-ray diffraction data.

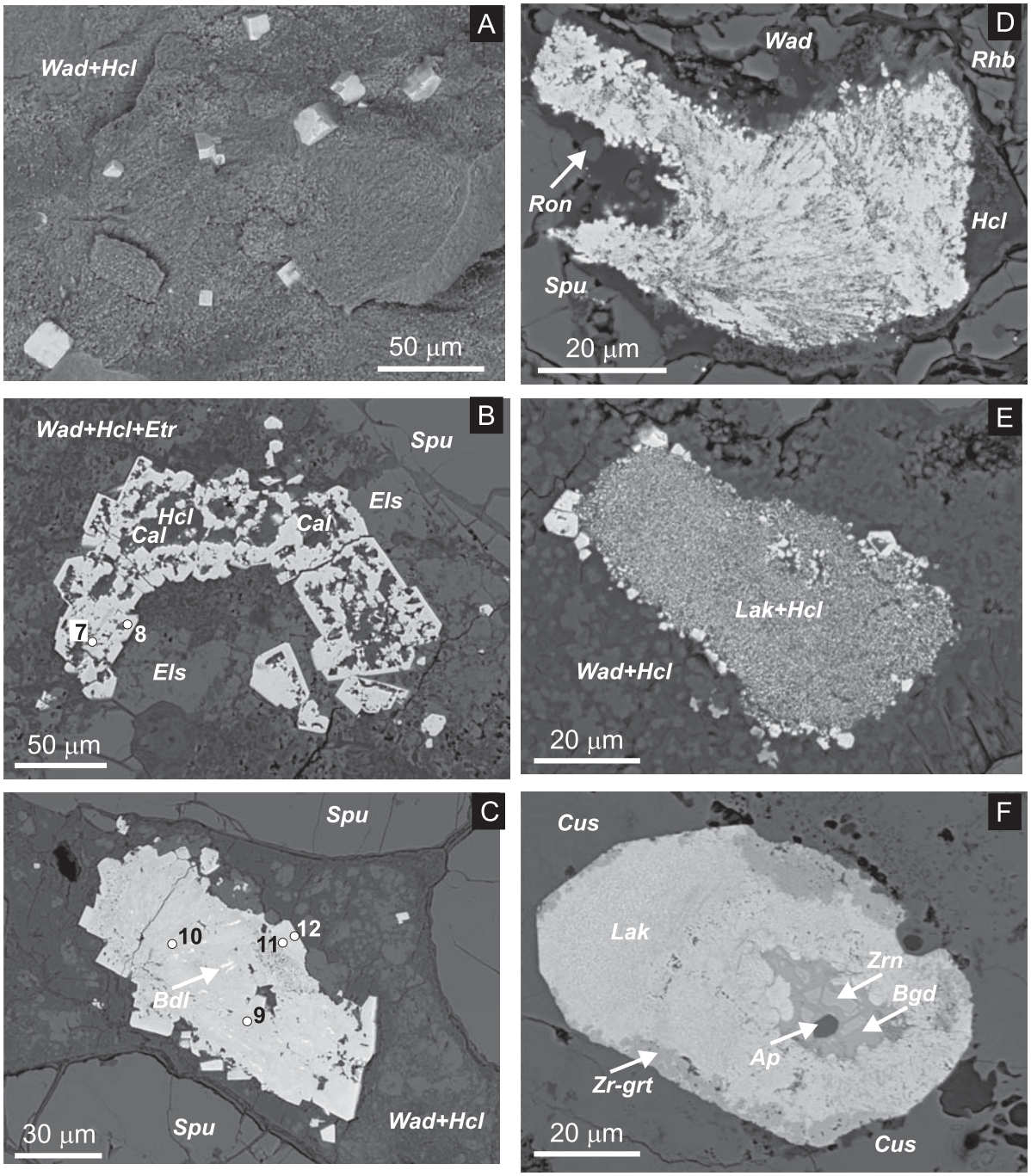

FIGURE 1. BSE image showing morphology of lakargiite aggregates (light). Points of microprobe analyses are shown. (**a**) Pseudocubic crystals in fine-grained wadalite-hydrocalumite mass. (**b**) Skeletal crystal growth. (**c**) Regenerated inhomogeneous spherule-like aggregate with baddeleyite relics. (**d**) Dendroid spherule. (**e**) Framboidal-like aggregate overgrown by larger crystals (fragment of lakargiite-hydrocalumite intergrowth with grain size of ca. 500 nm). (**f**) Pseudomorph of lakargiite after zircon. Lak = lakargiite, Wad = wadalite, Hcl = hydrocalumite, Spu = spurrite, Els = hydroxylellestadite, Ron = rondorfite, Rhb = reinhardbraunsite, Cus = cuspidine, Bdl = baddeleyite, Etr = mineral of ettringite group, Zrn = zircon, Bgd = baghdadite-like mineral, Zr-grt = kimzeyite-like mineral, Ap = apatite.

As its synthetic analog, lakargiite is biaxial and optically positive. Definition of the optical properties of lakargiite is inhibited by strong twinning and small crystal size. Sectoral twinning is well observed using crossed polars and compensator: sectors oblique to one another in a pseudocubic crystal show different interference colors. Lakargiite forms twins according to the following twin laws: 90° rotation around [101] and 180° rotation around [101] (Dravid et al. 1989; Keller and Buseck 1994). Refractive indices, determined in a mixture of sulfur and selenium are $\alpha = 2.1(1)$, $\beta = 2.1(1)$, $\gamma = 2.1(1)$ (589 nm). Identical refractive indices measured along different crystallographic directions reflect difficulties in measuring high refractive

TABLE 1. Chemical composition of lakargiite and perovskite from Lakargi Mountain (North Caucasus)

wt%	1	s.d.	Range	2	3	4	5	6	7	8	9	10	11	12	13
UO_3	2.24	0.38	0.81–2.78	1.84	0.86	4.05	0.10	n.d.	1.66	3.08	1.05	0.58	2.84	2.66	n.d.
Nb_2O_5	0.56	0.07	0.40–0.75	0.64	0.40	0.54	0.10	2.85	1.15	0.58	0.13	0.17	0.75	0.56	0.55
Ta_2O_5	0.09	0.03	0.05–0.14	0.11	0.12	0.06	n.d.	0.19	0.06	0.11	0.05	0.06	0.09	0.11	n.d.
ZrO_2	40.34	0.72	39.13–42.12	39.19	40.96	43.54	64.35	35.07	55.17	41.58	57.05	60.59	40.42	44.18	1.48
SnO_2	11.14	1.27	9.55–16.19	10.93	16.19	10.58	0.66	16.23	0.87	10.22	0.12	2.91	7.32	9.48	0.35
TiO_2	7.89	0.98	4.98–9.66	9.66	4.98	5.89	1.06	7.67	4.60	6.10	2.30	1.25	10.03	6.30	51.32
HfO_2	0.90	0.04	0.78–1.01	0.88	1.01	0.80	1.20	0.65	0.99	0.81	1.48	1.07	0.83	0.93	0.07
ThO_2	0.84	0.17	0.52–1.09	0.73	1.02	0.62	0.07	0.42	0.02	0.53	n.d.	n.d.	0.26	0.34	0.13
SiO_2	0.04	0.03	0–0.11	n.d.	n.d.	0.11	0.26	n.d.	0.39	0.43	1.27	0.27	n.d.	n.d.	0.14
Fe_2O_3	2.46	0.30	1.74–3.05	2.59	1.74	2.37	0.72	3.71	1.74	2.02	2.24	0.36	2.84	1.75	3.92
Sc_2O_3	0.38	0.03	0.32–0.47	0.34	0.33	0.51	n.d.	0.12	0.03	0.61	0.05	0.06	0.37	0.37	n.d.
Cr_2O_3	0.34	0.06	0.17–0.46	0.38	0.17	0.25	n.d.	n.d.	n.d.	0.27	n.d.	0.03	0.32	0.28	0.41
Al_2O_3	0.04	0.01	0.02–0.08	0.04	0.03	0.03	0.23	0.03	0.01	0.06	0.04	n.d.	n.d.	n.d.	0.28
Ce_2O_3	0.53	0.08	0.29–0.68	0.54	0.29	0.48	n.d.	0.37	n.d.	0.43	n.d.	0.17	0.60	0.34	0.81
La_2O_3	0.58	0.12	0.25–0.84	0.56	0.25	0.51	n.d.	0.28	n.d.	0.50	n.d.	0.05	0.70	0.57	0.24
Nd_2O_3	0.14	0.09	0–0.34	0.25	0.26	0.05	n.d.	n.d.	n.d.	n.d.	n.d.	n.d.	0.16	0.11	n.d.
CaO	31.08	0.34	30.61–31.71	31.51	30.73	30.95	31.26	31.08	31.87	30.92	32.42	30.86	31.74	31.13	40.26
SrO	0.10	0.02	0.05–0.13	0.08	0.09	0.11	0.28	n.d.	0.20	0.12	0.22	0.25	0.09	0.10	0.11
MgO	0.01	0.005	0.01–0.02	0.02	0.01	0.01	n.d.	n.d.	n.d.	n.d.	0.03	0.01	n.d.	n.d.	n.d.
Total	99.70	0.72	98.53–101.26	100.29	99.44	101.41	100.29	98.67	98.74	98.37	98.57[1]	98.69	99.34[2]	99.13[3]	100.29[4]
Calculated on 2 cations															
Ca	0.985			0.982	0.996	0.983	0.991	0.988	1.006	0.996	1.017	1.001	0.989	0.997	0.989
Sr	0.002			0.001	0.002	0.002	0.005		0.003	0.002	0.004	0.004	0.002	0.002	0.001
Mg				0.001							0.001				0.001
Y											0.002				
Ce^{3+}	0.006			0.006	0.003	0.005		0.004		0.005		0.002	0.006	0.004	0.007
La^{3+}	0.006			0.006	0.003	0.006		0.003		0.006		0.001	0.008	0.006	0.002
Nd^{3+}	0.001			0.003	0.003								0.002		
Th	0.006			0.005	0.007	0.004		0.003		0.004	0.001		0.002	0.002	0.001
A site	*1.006*			*1.004*	*1.014*	*1.000*	*0.996*	*0.998*	*1.009*	*1.013*	*1.025*	*1.008*	*1.009*	*1.011*	*1.001*
Zr	0.582			0.555	0.604	0.629	0.928	0.506	0.793	0.609	0.815	0.895	0.573	0.644	0.017
Hf	0.008			0.007	0.009	0.007	0.010	0.006	0.008	0.007	0.012	0.009	0.007	0.008	
Sn	0.131			0.127	0.195	0.125	0.008	0.192	0.010	0.122	0.001	0.035	0.085	0.113	0.003
Ti^{4+}	0.176			0.211	0.113	0.131	0.024	0.171	0.103	0.138	0.051	0.028	0.219	0.142	0.884
Si	0.001					0.003	0.008		0.011	0.013	0.037	0.008			0.003
Fe^{3+}	0.055			0.057	0.040	0.053	0.016	0.083	0.039	0.046	0.049	0.008	0.062	0.039	0.068
Nb^{5+}	0.007			0.008	0.005	0.007	0.001	0.038	0.015	0.008	0.002	0.002	0.010	0.008	0.006
Ta^{5+}	0.001			0.001	0.001			0.002	0.001	0.001			0.001	0.001	
U^{6+}	0.014			0.011	0.005	0.025	0.001		0.010	0.019	0.006	0.004	0.017	0.017	
Sc	0.010			0.009	0.009	0.013		0.003	0.001	0.016	0.001	0.002	0.009	0.010	
Cr^{3+}	0.008			0.009	0.004	0.006				0.006		0.001	0.007	0.006	0.007
V^{3+}															0.003
Al	0.001			0.001	0.001	0.001	0.008	0.001		0.002	0.001				0.008
B site	*0.994*			*0.996*	*0.986*	*1.000*	*1.004*	*1.002*	*0.991*	*0.987*	*0.975*	*0.992*	*0.991*	*0.989*	*0.999*
Δe^+	0.025			0.027	0.043		0.013	0.030	0.022	0.030	0.124	0.014	0.035	0.018	0.065

Notes: 1–4 = small single lakargiite crystals (20–30 μm): 1 = average composition based on 24 analyses of the crystals used for structural research and optical measurements; 2 = crystal with greatest Ti content; 3 = crystal with greatest Sn content; 4 = crystal with biggest U content; 5, 6 = granular aggregate with maximum Zr content: 5 = core, 6 = rim; 7, 8 = intergrowths of skeletal crystals, points of the analysis are shown on Figure 1b; 9–12 = heterogeneous spherulite-like aggregate with baddeleyite relics, points of the analysis are shown on Figure 1c; 13 = perovskite grain (30 μm). Δe^+ = deficit in positive charge possibly specifying presence of OH groups, in total, wt%: [1]0.02 V_2O_3 and 0.10 Y_2O_3; [2]0.02 MnO; [3]0.03 V_2O_3; [4]0.04 MnO and 0.18 V_2O_3.

indices for a twinned pseudocubic mineral. A mean refractive index calculated from the empirical formula and density yielded 2.002. The birefringence is less than 0.003–0.005, measured $2V$ is close to 0°, and the crystallographic orientation is: X = *a*, Y = *c*, Z = *b*.

Based on the empirical formula and calculated density, the compatibility index $1 - (K_p/K_C) = -0.074$ is only fair (Mandarino 1981) because of small crystal size, wide compositional variations, twinning, and the difficulty of precisely measuring the refractive indices.

Lakargiite belongs to the ternary solid solution $CaZrO_3$-$CaTiO_3$-$CaSnO_3$ (lakargiite-perovskite-unnamed end-member, synthetic phase). The content of $CaZrO_3$ reaches 93%, the maximum content of $CaTiO_3$ is 22%, and that of $CaSnO_3$ is about 20% (Table 1). In addition, significant amounts of U, Th, Hf, Nb, Fe, Cr, Sc, Ce, and La characterize lakargiite (Table 1). The composition of lakargiite with high content of uranium indicates that uranium as U^{6+} is probably incorporated at the zirconium site (Table 1).

Compositional data of lakargiite plot into one field with different compositional trends (Fig. 2). Small individual crystals (the crystals used for the structural and optical studies) with insignificant core-to-rim increase in Zr and Sn contents group in one field (trend marked 4 in Fig. 2). Lakargiite as irregular spherulite-like and dendroid aggregates is characterized by high $CaZrO_3$ contents, and with baddeleyite relics in their cores, plot on the other trend (marked 3); thin margins of these are enriched in Sn, Ti, and Nb (Table 1; Figs. 1c and 2). The later, high-Sn zones in small crystals have relatively low contents of Nb and Ti, which most probably reflects the synchronous growth of these zones with perovskite and the potentially new mineral $Ca_3Fe_2TiO_8$ during the progressive contact-metamorphic stage.

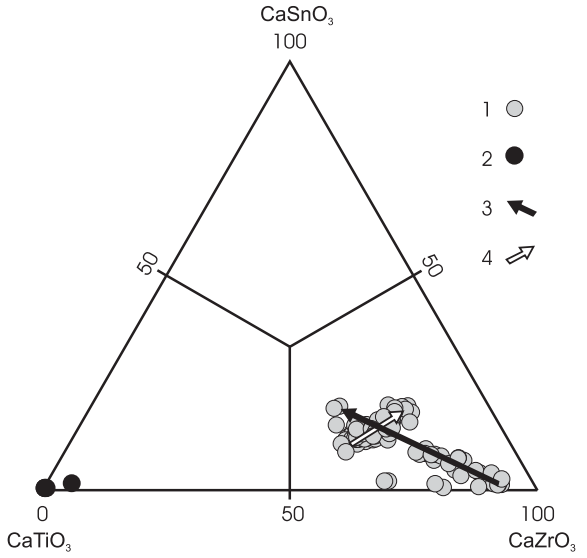

FIGURE 2. Points of analyses of (1) lakargiite and (2) perovskite from the Caucasus plotted on the classification diagram $CaTiO_3$-$CaSnO_3$-$CaZrO_3$. (3) Changing compositional trend of irregular and deformed aggregates of lakargiite. (4) Changing compositional trend of small idiomorphic crystals of lakargiite.

The development of reactive rims on grain and spherulite-like aggregates of lakargiite with relatively high content of Sn, Ti, and Nb is probably due to regressive compositional changes in perovskites (Table 1; Fig. 2).

The cation charge may indicate a negligible content of OH groups—as confirmed by IR data (Table 1). This phenomenon, typical of natural perovskites (Beran et al. 1996), has been used successfully in the synthesis of proton conductors (Iwahara 1996; Shi et al. 2005). It must be noted that other Ca-mineral nano-inclusions (<100–200 nm) may have influenced the quality of the lakargiite microprobe analyses.

All of the seven lakargiite crystals examined with a single-crystal X-ray diffractometer (<30 μm in maximum dimension) were intimately twinned and, thus, could not be used for structure refinement. However, reflection splitting indicated that lakargiite is an orthorhombic perovskite, confirmed by optical observations. Orthorhombic lakargiite unit-cell parameters were obtained by way of transformation of a cubic model ($Pm\bar{3}m$) with a = 3.965(4) Å and V = 62.35(11) Å^3, modified by the separation of split reflections due to pseudocubic twinning, leading to space group *Pbnm* with a = 5.55(2), b = 5.65(2), c = 7.93(2) Å, V = 248.7(2) Å^3, Z = 4.

Powder X-ray diffraction data refined in space group *Pbnm* yielded a = 5.556(1), b = 5.715(1), c = 7.960(1) Å, V = 252.7(1) Å^3, Z = 4. Measured and fitted powder diffraction data, difference plot, and positions of the diffracted lines are displayed on Figure 3. Rietveld R-factors were: R_p = 8.44%, R_{wp} = 12.85%, and R_{exp} = 0.85%. Cell parameters refined on the basis of powder X-ray data (Table 2) are larger than those derived by the single-crystal method. This is probably due to the relatively higher $CaZrO_3$ content in the aggregates used for the powder measurement (Table 1; Fig. 2).

In general, lakargiite cell dimensions are smaller than those of synthetic $CaZrO_3$ (Koopmans et al. 1983: a = 5.5912, b = 5.76165, c = 8.0171 Å; *Pbnm*). This is due to a solid solution of lakargiite with $CaTiO_3$ (Koopmans et al. 1983: a = 5.3829, b = 5.4458, c = 7.6453 Å; *Pbnm*), and $CaSnO_3$ [Kung et al. 2001: a = 5.5133(1), b = 5.6630(2), c = 7.8807(3) Å; *Pbnm*]. Unit-

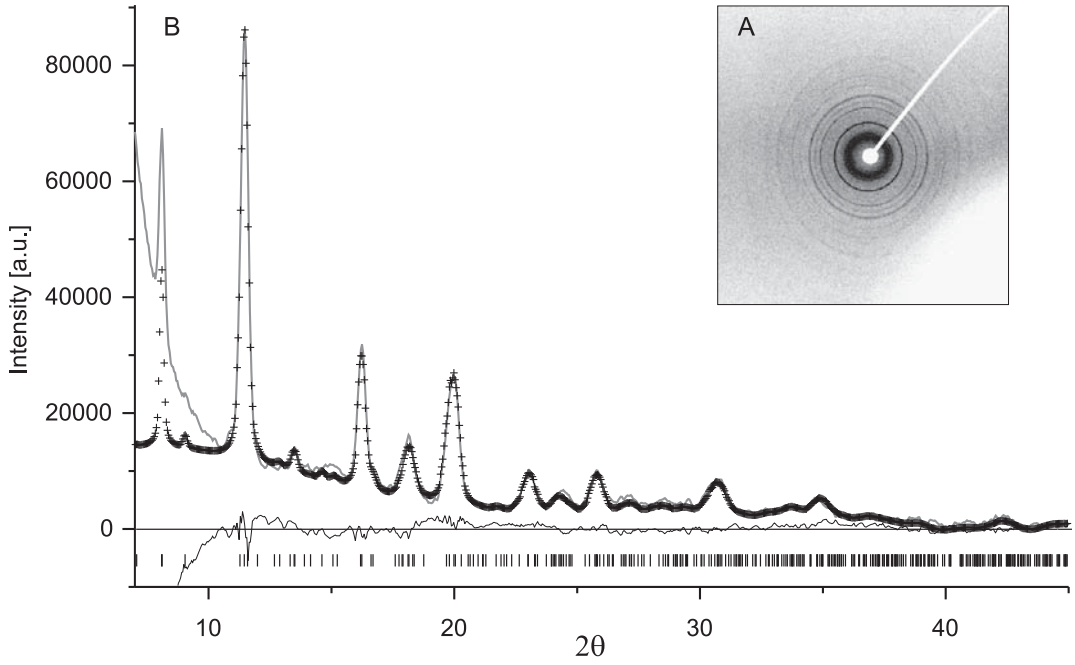

FIGURE 3. (**a**) Two-dimensional XRD image of lakargiite powder sample. (**b**) Measured (solid line), fitted (+) pattern, and a difference plot between observed and calculated diffraction lines of lakargiite.

TABLE 2. X-ray powder diffraction data of lakargiite

hkl	Measured		Calculated		*hkl*	Measured		Calculated	
	d (Å)	*I*	*d* (Å)	*I*		*d* (Å)	*I*	*d* (Å)	*I*
101		<1	4.559	0.2	314	1.318	3	1.319	2.1
110	3.970	28	3.985	25.4	402	1.312	2	1.311	1.9
002	3.964	12	3.979	11.2	240	1.268	5	1.271	3.7
111	3.544	3	3.563	2.8	332	1.258	7	1.260	7.9
020	2.850	25	2.857	24.9	116	1.256	10	1.259	10.5
112	2.807	100	2.816	100.0	420	1.248	4	1.249	4.1
200	2.771	22	2.778	22.1	242	1.209	4	1.210	3.3
021		<1	2.689	0.4	422	1.191	5	1.192	2.6
120	2.537	<1	2.541	0.5	044	1.160	1	1.161	3.5
210	2.492	1	2.498	1.3	243	1.145	1	1.146	1.3
121	2.414	1	2.421	1.2	404	1.138	3	1.139	3.7
103	2.389	3	2.394	2.9	150	1.119	2	1.120	1.8
211	2.376	3	2.384	2.9	334	1.105	2	1.105	1.8
022	2.310	1	2.321	0.8	152	1.077	3	1.078	2.9
202	2.273	1	2.278	1.1	244	1.073	5	1.071	4.6
113	2.211	2	2.208	2.5	136	1.067	5	1.068	4.6
122	2.137	2	2.142	1.5	316	1.058	6	1.060	6.7
212	2.112	<1	2.116	0.6	424	1.057	5	1.058	5.1
220	1.988	34	1.992	32.6	512	1.050	8	1.052	6.8
004	1.980	15	1.990	17.7	440	0.996	3	0.996	1.6
023	1.926	1	1.944	1.6	154	0.976	1	0.976	2.6
221	1.923	3	1.932	2.1	350	0.972	1	0.973	1.7
123	1.833	<1	1.835	0.5	442	0.965	3	0.966	2.2
213	1.816	<1	1.819	0.5	352	0.945	3	0.945	3.1
130	1.808	8	1.802	7.6	028	0.940	3	0.940	3.0
222	1.780	9	1.781	9.8	336	0.939	4	0.939	4.1
114	1.776	9	1.780	8.1	208	0.937	3	0.937	2.9
310	1.767	3	1.762	3.0	532	0.933	5	0.933	4.7
131	1.747	3	1.757	3.9	062	0.926	2	0.926	1.5
311	1.718	<1	1.720	0.7	246	0.918	2	0.918	1.6
132	1.640	18	1.642	21.2	444	0.890	2	0.891	2.1
024	1.631	14	1.633	14.5	228	0.889	2	0.890	2.8
204	1.616	12	1.618	13.8	620	0.880	1	0.881	1.2
312	1.610	36	1.611	31.0	262	0.878	2	0.879	2.0
320	1.552	<1	1.554	0.3	354	0.873	2	0.874	1.8
105	1.528	<1	1.530	0.3	156	0.855	1	0.856	1.6
133	1.497	<1	1.491	1.6	516	0.842	5	0.843	3.5
040	1.426	4	1.429	3.9	604	0.839	2	0.840	1.3
224	1.405	18	1.408	17.5	624	0.805	2	0.806	1.9
041	1.404	1	1.406	0.7	248	0.783	2	0.783	1.7
400	1.387	5	1.389	3.9	428	0.778	2	0.778	1.9
140	1.382	<1	1.384	0.5	536	0.777	2	0.778	1.7
233	1.350	<1	1.352	0.5	712	0.771	2	0.771	2.2
410	1.348	<1	1.350	0.3	462	0.771	1	0.771	1.4
125	1.348	<1	1.349	0.5	642	0.763	2	0.763	0.9
042	1.344	2	1.345	2.6	174	0.749	1	0.748	1.5
215	1.341	<1	1.343	0.5	266	0.745	1	0.745	1.3
134	1.332	5	1.336	5.1	158	0.744	1	0.744	1.1

cell parameters and content of $CaTiO_3$ in synthetic perovskites $CaZr_{1-x}Ti_xO_3$ are inversely related (Levin et al. 2006). Structural and optical investigations did not show any metamictization of lakargiite, though rich in U and Th.

The crystal structure of the synthetic lakariite analog, $CaZrO_3$ (orthorhombic Zr perovskite, *Pbnm* in standard setting), is known (Koopmans et al. 1983). The perovskite framework structure is built of interconnected, apex-sharing Zr-octahedra, thus producing a distorted channel system occupied by Ca atoms. The deviation from an ideal cubic structure, an example of which is tausonite $SrTiO_3$, is defined by rotation of the Zr-octahedra (Glazer 1972; Mitchell 1996, 2002; Ross and Chaplin 2003; Shi et al. 2005).

A strong band near 523 cm^{-1} (Fig. 4a), characteristic of synthetic $CaZrO_3$ (Orera et al. 1998), is also seen in lakargiite IR spectra obtained using the ATR accessory in the range 400–900 cm^{-1}. A weak, broad band near 3340 cm^{-1} appears in the OH-region (Fig. 4b) that is probably related to incorporation

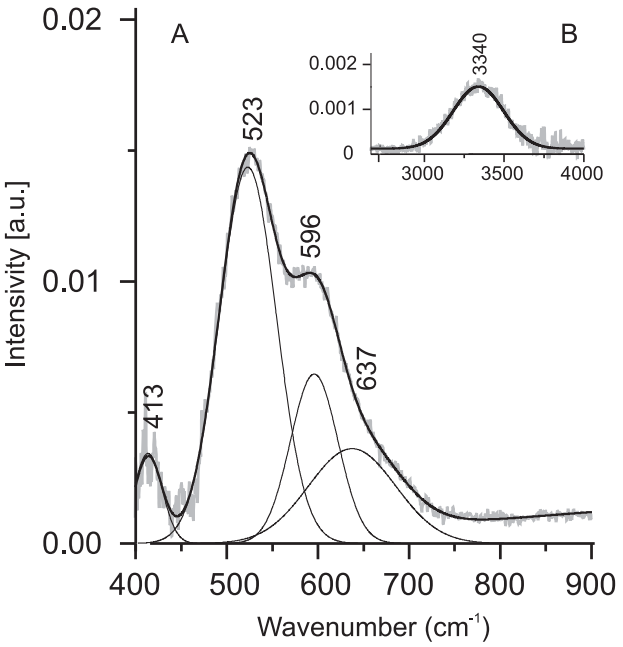

FIGURE 4. Infrared spectra of lakargiite for the (**a**) 400–900 cm^{-1} and (**b**) 2740–4000 cm^{-1} regions.

of trivalent cations according to the scheme $Zr + O^{2-} \rightarrow R^{3+} + OH^-$ (Yugami et al. 1996) or the appearance of vacancies at the Ca site, $Ca + 2O^{2-} \rightarrow \square + 2OH^-$ (Beran et al. 1996).

Lakargiite Raman spectra (Fig. 5) are analogous to those of the synthetic phase $CaZr_{1-x}Ti_xO_3$ where x = 0.08–0.17 (Levin et al. 2006) and are similar to the spectra of synthetic $CaZrO_3$ (McMillan and Ross 1988; Orera et al. 1998). The following modes are active in the spectra: 315, 335, **352**, 372, 391, 430, **437**, **446**, 520, **554**, 695, and **748** cm^{-1} (strong bands are in bold, Fig. 5).

CONCLUDING REMARKS

The parageneses of lakargiite with spurrite, larnite, calcio-olivine, rondorfite, ellestadite, and wadalite characterize extremely high-temperature metamorphism, at the lowest pressures in the sanidinite facies and in the larnite-merwinite depth facies of carbonate-rich rocks (Zharikov and Shmulovich 1969; Reverdatto 1970; Pertsev 1977; Korzhinskii 1993; Zharikov et al. 1998; Gazeev et al. 2006; Callegari and Pertsev 2007). Carbonate-silicate hornfelses and skarns of this kind are associated with subvolcanic or volcanic contacts with carbonate or silicate-carbonate rocks, and especially in xenoliths (Reverdatto 1970; Kanazawa et al. 1997; Mihajlović et al. 2004; Grapes 2006; Galuskin et al. 2007). The temperature of interaction of the calcareous rocks with peridotitic- and basic-magma can reach ca. 900–1000 °C, and ca. 800 °C at contacts with granitoid magmas. The evaluated CO_2 pressure falls in the range 10–200 × 10^5 Pa (Pertsev 1977, 1998).

The anomalously high (800–1000 °C) temperature of formation of the lakargiite skarns is probably related to "overheating" of acid lava within volcanic pipes, the walls of which contained the source material of the xenoliths (Babansky et al. 1995; Gazeev et al. 2006). Under laboratory conditions crystallization

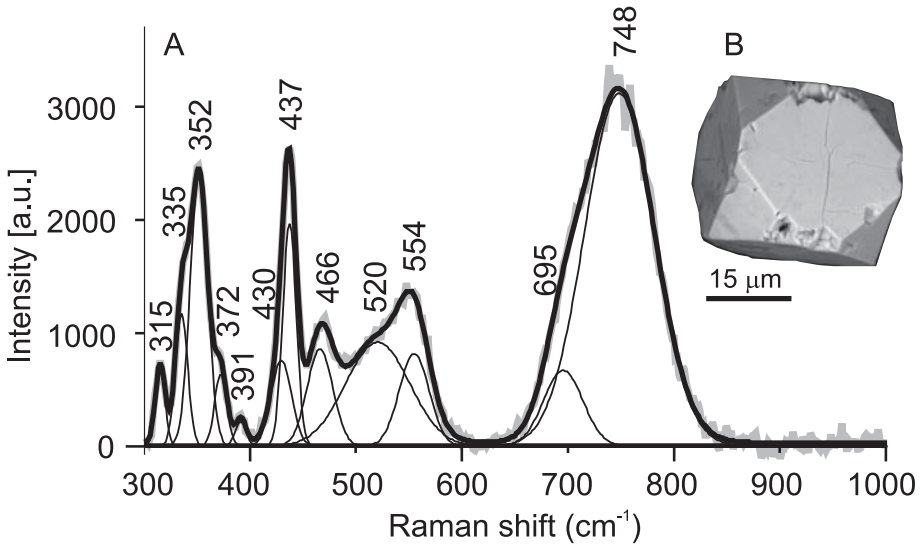

FIGURE 5. (**a**) Raman spectrum of lakargiite for the region 300–1000 cm^{-1} received from the (**b**) pseudocubic twinned crystals showing {100} + {111}, BSE image, low vacuum (0.2 Torr), without coating.

of $CaZrO_3$ in the system ZrO_2-$CaCl_2$-Na_2CO_3 at normal pressure begins at 700 °C with a liquid phase present (Li et al. 2007). Synthesis of $CaZrO_3$ in the absence of a liquid phase occurs only above 1100 °C (Yeo et al. 2004; Park 2007). Such high formation temperatures probably explain why lakargiite is so rare in comparison to $CaTiO_3$ perovskite. Another reason for its rarity may be that the high CaO content requires an extremely low CO_2 fugacity in any coexisting fluid to prevent carbonatization.

Combined high temperature, low pressure, high ZrO_2, and CaO activities can possibly exist only at contacts between silicate volcanic- and carbonate-rocks. A solid solution with $CaTiO_3$ and even trace contents of Cl, F, and S in the reaction medium will lower the temperature of $CaZrO_3$ synthesis (Lee et al. 2005; Pollet et al. 2005; Park 2007). These volatile elements are also agents of Zr fluid transport (Gonenli and Tas 1999). Relics of baddeleyite and zircon in lakargiite crystals reflect the early growth of Zr-minerals. Low SiO_2 activity prevented the formation of zircon in the carbonate xenoliths.

The high concentration of U and Th in lakargiite with an age <2.5–2.8 Ma and no traces of structural metamictization, may allow the future use of lakargiite in modeling of materials used for the immobilization of radioactive waste.

ACKNOWLEDGMENTS

We express our thanks to Roger Mitchell and Sergey Britvin for the constructive reviews and comments. Pádhraig Kennan helped with English. Financial support for this project was provided partly by the Scientific Research fund of the Polish Ministry of the Science and Higher Education grant N307 3531 33 and Russian Foundation Base Researches (RFBR), Project 08-05-00181a. X-ray diffraction experiments, performed on Rigaku D/max RAPID II diffractometer, were financed partly by European Regional Development Fund (ERDF).

REFERENCES CITED

Babansky, A.D., Ashichmina, N.A., Kovalenko, V.I., Lyatifova, E.N., and Kononkova, N.N. (1995) Initial magma of Upper-Chegem caldera complex rocks (North Caucasus) on research data of inclusions in minerals. Doklady Russian Academy of Sciences, 344, 226–228 (in Russian).

Beran, A., Libowitzky, E., and Armbruster, T. (1996) A single-crystal infrared spectroscopic and X-ray-diffraction study of untwinned San Benito perovskite containing OH groups. Canadian Mineralogist, 34, 803–809.

Borsuk, A.M. (1979) Mesozoic and Cainozoic magmatic formations of Caucasus Mountains, 299 p. Moscow, Nauka (in Russian).

Callegari, E. and Pertsev, N. (2007) Contact metamorphic and associated rocks. In D. Fettes and J. Desmons, Eds., Metamorphic Rocks: A Classification and Glossary of Terms, p. 69–81. Cambridge University Press, New York.

Chakhmouradian, A.R. (2006) High-field-strength elements in carbonatitic rocks: Geochemistry, crystal chemistry, and significance for constraining the sources of carbonatites. Chemical Geology, 235, 138–160.

Chakhmouradian, A.R., Yakovenchuk, V., Mitchell, R.H., and Bogdanova, A. (1997) Isolueshite: a new mineral of the perovskite group from Khibina alkaline complex. European Journal of Mineralogy, 9, 483–490.

Dravid, V.P., Sung, C.M., Notis, M.R., and Lyman, C.E. (1989) Crystal symmetry and coherent twin structure of calcium ziconate. Acta Crystalographica, B45, 218–227.

Galuskin, E.V., Pertsev, N.N., Armbruster, T., Kadiyski, M., Zadov, A.E., Galuskina, I.O., Dzierżanowski, P., Wrzalik, R., and Kislov, E. (2007) Dovyrenite $Ca_6Zr[Si_2O_7]_2(OH)_4$—a new mineral from skarned carbonate xenoliths in basic-ultrabasic rocks of the Ioko-Dovyren Massif, Northern Baikal Region, Russia. Mineralogia Polonica, 38, 15–28.

Gazeev, V.M., Zadov, A.E., Gurbanov, A.G., Pertsev, N.N., Mokhov, A.V., and Dokuchaev, A.Ya. (2006) Rare minerals of Verkhniy Chegem caldera (in skarned carbonates xenoliths in ignimbrites). Vestnik Vladikavkazskogo Nauchnogo Centra, 6, 18–27 (in Russian).

Glazer, A.M. (1972) The classification of tilted octahedra in perovskites. Acta Crystalographica, B28, 3384–3392.

Gonenli, I.E. and Tas, G. A. (1999) Chemical synthesis of pure and Gd-doped $CaZrO_3$ powders. Journal of European Ceramic Society, 19, 2563–2567.

Grapes, R. (2006) Pyrometamorphism, 275 p. Springer, Berlin.

Iwahara, H. (1996) Proton conducting ceramics and their applications. Solid State Ionics, 86–88, 9–15.

Kanazawa, Y., Aoki, M., and Takeda, H. (1997) Wadalite, rustumite, and spurrite from La Negra mine, Queretaro, Mexico. Bulletin of Geological Survey of Japan, 48, 413–420.

Keller, L.P. and Buseck, P.R. (1994) Twinning in meteoritic and synthetic perovskite. American Mineralogist, 79, 73–79.

Konev, A.A. and Samoilov, V.S. (1974) Contact metamorphism and metasomatism in aureole of Tazheran alcalic intrusive, 245 p. Nauka, Novosibirsk (in Russian).

Koopmans, H.J.A., van de Velde, G.M.H., and Gellings, P.J. (1983) Powder neutron diffraction study of the perovskites $CaTiO_3$ and $CaZrO_3$. Acta Crystallographica, C39, 1323–1325.

Korzhinskii, D.S. (1993) Factors of mineral equilibria and mineralogical facies of depths. In V.A. Zharikov, Ed., Korzhinskii's Selected Papers: Petrology of Metamorphism, p. 56–145. Nauka, Moscow (in Russian).

Kraus, W. and Nolze, G. (1996) POWDER CELL—a program for the representation and manipulation of crystal structures and calculation of the resulting X-ray powder patterns. Journal of Applied Crystallography, 29, 301–303 (ftp://ftp.bam.de/Powder_Cell/).

Kung, J., Angel, R.J., and Ross, N.L. (2001) Elasticity of $CaSnO_3$ perovskite. Physics and Chemistry of Minerals, 28, 35–43.

Kuznetsov, I.G. (1925) Loparite—a new rare earth mineral from the Khibina Tundra. Izvestia Geologicheskogo Komiteta, 44, 663–682 (in Russian).

Lee, W.-J., Wakahara, A., and Kim, B.-H. (2005) Decreasing of $CaZrO_3$ sintering temperature with glass frit addition. Ceramic International, 31, 521–524.

Levin, I., Cockayne, E., Lufaso, M.W., Woicik, J.C., and Maslar, J.E. (2006) Local structures and Raman spectra in the $Ca(Zr,Ti)O_3$ perovskite solid solutions. Chemistry of Materials, 18, 854–860.

Li, Z., Lee, W.D., and Zhang, S. (2007) Low-temperature synthesis of $CaZrO_3$ powder from molten salts. Journal of American Ceramic Society, 90, 364–368.

Lipman, P.W., Bogatikov, O.A., Tsvetkov, A.A., Gazis, C., Gurbanov, A.G., Hon, K., and Koronovsky, N.V. (1993) 2.8 Ma ash-flow caldera at Chegem River in the Northern Caucasus Mountain (Russia), cotemporaneous granites and associated ore deposits. Journal of Volcanology and Geothermal Researches, 57, 85–124.

Lumpkin, G.R. (2001) Alpha-decay damage and aqueous durability of actinide host phases in natural systems. Journal of Nuclear Materials, 289, 136–166.

Lupini, L., Williams, C.T., and Woolley, A.R. (1992) Zr-rich garnet and Zr- and Ti-rich perovskite from the Polino carbonatite, Italy. Mineralogical Magazine, 56, 581–586.

Ma, C. and Rossman, G.R. (2008) $BaTiO_3$, a new mineral from the Benitoite Mine, California. American Mineralogist, 93, 154–157.

Mandarino, J.A. (1981) The Gladstone-Dale relationship. IV. The compatibility concept and its application. Canadian Mineralogist, 19, 441–450.

McMillan, P. and Ross, N. (1988) The Raman spectra of several orthorhombic calcium oxide perovskites. Physics and Chemistry of Minerals, 16, 21–28.

Mihajlović, T., Lengauer, C.L., Ntaflos, T., Kolitsch, U., and Tillmanns, E. (2004) Two new minerals, rondorfite, $Ca_8Mg\ [SiO_4]_4Cl_2$, and almarudite, $K(\square, Na)_2(Mn,Fe,Mg)_2(Be, Al)_3[Si_{12}O_{30}]$, and a study of iron-rich wadalite, $Ca_{12}[(Al_8Si_4Fe_2)O_{32}]Cl_6$, from the Bellerberg (Bellberg) volcano, Eifel, Germany. Neues Jahrbuch für Mineralogie Abhandlungen, 179, 265–294.

Milanovsky, E.E. and Koronovsky, N.B. (1973) Orogenic volcanism and tectonics of Eurasia Alpine belt, 278 p. Nedra, Moscow (in Russian).

Mitchell, R.H. (1996) Perovskites: a revised classification scheme for an important rare earth element host in alkaline rocks. In P. Jones, F. Wall, and T. Williams, Eds., Rare Earth Minerals: Chemistry, Origin and Ore Deposits, p. 41–76. Chapman and Hall, London.

——— (2002) Perovskites. Modern and Ancient, 317 p. Almaz Press, Thunder Bay, Ontario.

Nickel, E.H. (1964) Latrappite—a proposed new mineral name for the perovskite-type calcium niobate mineral from the Oka area of Quebec. Canadian Mineralogist, 7, 683–697.

Orera, V.M., Pecharroman, C., Peña, J.I., Merino, R.I., and Serna, C.J. (1998) Vibrational spectroscopy of $CaZrO_3$ single crystals. Journal of Physics: Condensed Matter, 10, 7501–7510.

Park, J.H. (2007) Formation of $CaZrO_3$ at the interface between $CaO\text{-}SiO_2\text{-}MgO\text{-}CaF_2(\text{-}ZrO_2)$ slags and magnesia refractories: Computational and experimental study. Computer Coupling of Phase Diagrams and Thermochemistry (CALPHAD), 31, 149–154.

Pekov, I. (1998) Minerals first discovered on the territory of the former Soviet Union, 370 p. Ocean Pictures, Moscow.

Pertsev, N.N. (1977) High temperature metamorphism and metasomatism of carbonate rocks, 255 p. Nauka, Moscow (in Russian).

——— (1998) Acidic-basic interaction of silicate magmas with carbonate rocks. Doklady of Earth Sciences, 362, 978–981.

Pollet, M., Marinel, S., and Roulland, F. (2005) High decreasing in $CaZrO_3$ sintering temperature using complex fluoride fluxes. Journal of European Ceramic Society, 25, 2773–2777.

Radusinović, D. and Markov, C. (1971) Macedonite—lead titanate: A new mineral. American Mineralogist, 56, 387–394.

Reverdatto, V.V. (1970) Facies of contact metamorphism, 270 p. Nedra, Moscow (in Russian)

Rose, G. (1839) Beschreibung eineiger neuer Mineralien vom Ural. Pogendorff Annalen der Physik und Chemie, 48, 551–572.

Ross, N.L. and Chaplin, T.D. (2003) Compressibility of $CaZrO_3$ perovskite: comparison with Ca-oxide perovskites. Solid State Chemistry, 172, 123–126.

Safiannikoff, A. (1959) Un nouveau mineral de niobium. Bulletin des Séances de l'Académie Royale des Sciences d'Outre-Mer, 5, 1251–1255.

Saxena, S.K., Dubrovinsky, L.S., Lazor, P., Cerenius, Y., Häggkvist, P., Hanfland, M., and Hu, J. (1996) Stability of perovskite ($MgSiO_3$) in the Earth's mantle. Science, 274, 1357–1359.

Shi, Ch., Yoshino, M., and Morinaga, M. (2005) First-principles study of protonic conduction in In-doped $AZrO_3$ (A = Ca, Sr, Ba). Solid State Ionics, 176, 1091–1096.

Yeo, J.-G., Choi, S.-Ch., Kim, J.-W., Lee, J.-E., Lee, J.-H., and Jung, Y.-G. (2004) Thermal reaction behavior of $ZrSiO_4$ and $CaCO_3$ mixtures for high-temperature refractory application. Materials Science and Engineering, A368, 94–102.

Yugami, H., Shibayama, Y., Matsuo, S., Ishigame, M., and Sin, S. (1996) Proton sites and defect-interaction in $SrZrO_3$ single crystals studies by infrared absorption spectroscopy. Solid State Ionics, 85, 319–322.

Vorob'ev, E.I., Konev, A.A., Malyshonok, Y.V., Afonina, G.G., and Sapozhnikov, A.N. (1984) Tausonite $SrTiO_3$ new mineral of the perovskite group. Zapiski Vsesoyuznogo Mineralogicheskogo Obschestva, 113, 86–89 (in Russian).

Zharikov, V.A. and Shmulovich, K.I. (1969) High-temperature mineral equilibrium in system $CaO\text{-}SiO_2\text{-}CO_2$. Geochemia, 9, 1039–1056 (in Russian).

Zharikov, V.A., Rusinov, V.L., Marakushev, A.A., Zaraysky, G.P., Omel'yanchenko, B.I., Pertsev, N.N., Rass, I.T., Andreeva, O.V., Abramov, C.C., and Podlesski, K.V. (1998) Metasomatism and metasomatic rocks, 489 p. Nauka, Moscow (in Russian).

MANUSCRIPT RECEIVED DECEMBER 19, 2007
MANUSCRIPT ACCEPTED MAY 28, 2008
MANUSCRIPT HANDLED BY SERGEY KRIVOVICHEV